Energy Conversion and Management 271 (2022) 116303

Contents lists available at ScienceDirect

Energy Conversion and Management

journal homepage: www.elsevier.com/locate/enconman

Floating wind turbine energy and fatigue loads estimation according to climate period scaled wind and waves

Aitor Saenz-Aguirre [a,*], Alain Ulazia [a], Gabriel Ibarra-Berastegi [b,c], Jon Saenz [c,d]

[a] Energy Engineering Department, University of the Basque Country (UPV/EHU), Otaola 29, 20600 Eibar, Spain
[b] Energy Engineering Department, University of the Basque Country (UPV/EHU), Alda, Urkijo, 48013 Bilbao, Spain
[c] Plentziako Itsas Estazioa (BEGIK), University of Basque Country (UPV/EHU), Areatza Hiribidea 47, 48620 Plentzia, Spain
[d] Department of Physics, University of the Basque Country (UPV/EHU), Sarriena, 48940 Leioa, Spain

ARTICLE INFO

Keywords:
Wind energy
Floating Offshore
Fatigue loads
Cluster analysis
ERA5

ABSTRACT

Offshore wind power is one of the fastest-growing renewable energy sources, as it is expected to play a major role in the transition towards sustainability and net zero emissions. Despite its potential, the interaction of the turbines with the oceanic waves, especially in case of floating turbines, is one of the main drawbacks associated to it. In fact, mechanical oscillations caused by the waves could potentially alter the operation and lifetime of the turbines. Hence, while the characterization of the wind is sufficient for the long-term design of onshore wind turbines, the procedure is more complex in case of offshore turbines, since the height, period and direction of the waves will affect the lifetime of the turbine. In this paper, a methodology for the evaluation of the energy generation and fatigue mechanical loads of a Floating Offshore Wind Turbine (FOWT) considering a 30-year period is proposed. To that end, meteorological data from 1991 to 2020 are characterized using a cluster analysis and reduced into a computationally affordable number of simulation cases. Results show negligible energy loss of a FOWT due to interaction with the oceanic waves. However, a substantial increment of the mechanical fatigue in the side-side and fore-aft bending moments of the tower are detected. Such analyses might be applied for the predictability of the lifetime of an offshore wind turbine, as well as the selection of potential optimal wind farm locations, based on climatic patterns and the evolution of meteorological data.

1. Introduction

The rapidly increasing number of offshore wind turbines is a clear representation of the growth of this technology in the recent years. After the installation of the first offshore turbine in 1990, the cumulative offshore wind power capacity had already incremented to 1471 MW by 2008 [1]. From that moment on, the tendency has been exclusively incremental and by 2017 a 1.5% (43 TWh) of the energy production in the European Union presented offshore wind origin [2]. The prognosis is the short-term expansion and settlement of marine renewable energy sources, especially wind and wave power, as the principal drivers of the decarbonization and net zero emission process in the energy generation infrastructure [3].

The main advantages of offshore wind power in comparison to onshore wind technology are related to the wind speed resource at oceanic locations [4], where usually higher mean wind speed values and lower turbulence and wind shear are found. Higher wind speed values allow improved energy generation, and lower turbulence is translated into a reduction of the mechanical loads in the wind turbine. Additionally, depending on the distance to the shore, offshore wind turbines are unrestricted in terms of visual or noise impact, which increases the availability of areas for the installation of wind turbines. Expensive foundations or mooring systems, costly maintenance, difficulties related to grid integration and hydrodynamic interaction with the ocean waves are the most important drawbacks associated to offshore wind technology. A detailed comparison between onshore and offshore wind technologies is provided in [1].

Concerning location, offshore wind turbines might be installed either near-shore or far-offshore [5]. Strict regulations in some countries, regarding noise or visual impact of the wind turbines, as well as the protection of near-shore marine ecosystems, have led to the installation of far-offshore wind farms, which, as a consequence of the larger water depth, require Floating Offshore Wind Turbines (FOWTs). Additionally, in some cases, the installation of FOWTs is a direct result of the abrupt coastal floor in some areas, where the large water depth near-shore prevents the installation of bottom-fixed wind turbines. In this context,

* Corresponding author.
E-mail address: aitor.saenz@ehu.eus (A. Saenz-Aguirre).

https://doi.org/10.1016/j.enconman.2022.116303
Received 23 July 2022; Received in revised form 27 September 2022; Accepted 28 September 2022
Available online 17 October 2022

List of Abbreviations

AEP	Annual Energy Production
CF	Capacity Factor
DEL	Damage Equivalent Load
DLC	Design Load Case
ECMWF	European Centre of Medium-Range Weather Forecasts
FAST	Fatigue, Aerodynamics, Structures and Turbulence
FOWT	Floating Offshore Wind Turbine
HAWT	Horizontal Axis Wind Turbine
LCA	Life Cycle Assessment
LSS	Low Speed Shaft
NREL	National Renewable Energies Laboratory
NTM	Normal Turbulence Model
SSP	Shared Socioeconomic Pathway
SWL	Surface Water Level
TMD	Tuned Mass Damper

Nomenclature

U_{10}	Wind speed at 10 m height from ERA5
U_{100}	Wind speed at 100 m height from ERA5
U_{90}	Wind speed at 90 m height
z_0	Roughness of the sea
$Udir$	Incoming direction of wind (degrees clockwise from North)
ρ_0	Standard air density
ρ	Real air density
H_s	Significant wave height
T_p	Peak wave period
$H_s dir$	Incoming direction of waves (degrees clockwise from North)
m	Material exponent for fatigue calculation
k	Weibull scale parameter
c	Weibull form parameter
P_U	Probability of occurrence of wind speed for the confidence interval of the centroid in each cluster
P_{st}	Standard probability of occurrence of wind speed for the confidence interval of the centroid in each cluster
P_c	Probability of occurrence of each cluster

bathymetry studies must be conducted to characterize the coastal floor prior to selection of offshore wind farm locations [6].

The location of a wind farm, near-shore or far-offshore, will affect the costs associated to it. A comparison between a 20 year long Life Cycle Assessment (LCA) of a far-offshore wind farm (formed by 40–50 FOWTs) [7] and the LCA of an equivalent near-shore wind farm formed by bottom-fixed wind turbines [8] indicate that the increased economical cost associated to materials, installation and maintenance of FOWTs is compensated by a higher capacity factor. As a result, the LCA and the environmental impact of the electricity generation is similar in both cases.

Besides installation, maintenance and structural design of the wind turbine, wind farm location will also have an impact on the operation and mechanical loading of the wind turbines, as a result of their interaction with the oceanic waves. Numerical methods to study these hydrodynamic processes have been widely studied in literature [9]. In addition, as a result of the mechanical oscillations generated by the waves, their influence on the performance of the turbine might be amplified in case of FOWTs [10]. This could lead to power losses due to platform-pitch interactions [11], excitation of mechanical frequencies of the wind turbine components or the reduction of the expected lifetime of these components due to fatigue failure [12]. Increasing the aerodynamic damping via control functionalities [11], or with the introduction of additional Tuned Mass Damper (TMD) [12] are solutions proposed and nowadays used for FOWTs.

Therefore, a previous assessment of the wind and wave resources [13], as well as their coupling [14], at potential wind farm installation locations is crucial as it can help characterize the effect of the environmental conditions on the performance of the wind turbines [14], the increment of their fatigue mechanical loads as a result of the hydrodynamic interaction with the oceanic waves at that specific location or even optimize maintenance procedures [15]. On that account, optimal locations for the installation of wind farms based on the evolution of historical meteorological data could be selected.

While the characterization of the wind results sufficient for the long-term design and analysis of onshore wind turbines, the procedure gets complicated in case of offshore turbines, since the height, period and direction of the predominant waves need to be considered for such long-term horizon analyses. In this paper, a methodology is proposed for the estimation of the energy generation and the fatigue mechanical loads of FOWTs at specific offshore locations and under consideration of climatological normal periods as time horizon used in the calculations. This methodology shall be valid to analyse the effect of long-term climate change patterns on the wind turbine energy generation and their fatigue mechanical loads, as well as the predictability of future mechanical fatigue affection of the wind turbines based on meteorological projections and the selection of optimal locations based on historical or projected evolutions of meteorological conditions.

In this case, the wind and wave energy resource are obtained using fifth generation *ERA5* Reanalysis [16] at the grid point closest to Hywind-Scotland [−1.5°E, 57.5°N], i.e. first floating wind farm in the world. The time resolution of this study is 1 h and the studied period is 30 years (1991–2020), that is, the database includes 262 968 hourly cases. The selection of this reference period (30 years of data starting in 1991) corresponds to the current guidelines by the World Meteorological Organization [17] in the definition of climatological standard normals. This is the same period currently used by major meteorological data providers such as the Copernicus Climate Change Service in their climatological analyses [18].

The wind turbine model used for the calculation of the mechanical loading is the baseline NREL 5 MW turbine with OC3-Hywind spar-type flotation system. This model is structured around the open-source aeroelastic model OpenFAST v2.6.0 [19] and presents the same flotation device as the wind turbines in the Hywind wind farm [20]. OpenFAST tool, developed by the National Renewable Energies Laboratory (NREL), combines aerodynamics, hydrodynamics for offshore structures, control and structural dynamics. It offers, hence, a high-detailed simulation environment for both onshore and offshore wind turbines, which have been widely-used and accepted in the literature [21].

Finally, on account of the high number of meteorological resource datapoints in a climatological normal period of 30 years (262 968 hourly cases) and the computational unfeasibility to simulate and post-process all the cases using a high-detailed wind turbine model such as OpenFAST, a characterization method of the climatological normal period into a reduced number of datapoints is proposed in this paper. Thus, hourly wind and wave data in Hywind have been classified into 20 clusters using Ward's minimum variance method [22]. Next, the atmospheric-sea combined state representing each of the clusters has been used for a simulation using the aeroelastic code OpenFAST in order to analyse the operation and calculate the power production and the mechanical loads of a FOWT operating at such environmental conditions.

Table 1
Main characteristics of the baseline NREL 5 MW wind turbine.

	Value	Unit
Rated power	5	MW
Rotor diameter	123	m
Hub height, diameter	90, 3	m
Cut-in, rated, cut-out wind speed	3, 11.4, 25	m/s
Cut-in, rated rotor speed	6.9, 12.1	rpm

Table 2
Main characteristics of the OC3-Hywind spar-type flotation system.

	Value	Unit
Technology	Spar	–
Depth to platform base below SWL	120	m
Depth to anchors below SWL	320	m
Number of mooring lines	3	–
Platform mass, including ballast	7466.33	tonnes
Water displaced volume	8029	m^3

The paper is structured as follows: The wind and wave energy resource data and the analysis method of *ERA5* are introduced in Section 2.1. The wind turbine model and the simulation environment used in the analysis are described in Section 2.2. In Section 2.3 a detailed explanation of the methodology followed by the characterization of the climatological normal period using a cluster analysis and the calculation of the power production and the fatigue mechanical loads of the FOWT is given. In Sections 3 and 4, the results and discussion are presented, respectively. Finally, the conclusions and the future outlook are explained in Section 5.

2. Data and methodology

The wind and wave data used in the analysis and the methodology for the assessment of the power production and the fatigue mechanical damage in a FOWT over a climatological normal period are described in the following sections.

2.1. ERA5 reanalysis at Hywind-Scotland location

The fifth generation *ERA5* Reanalysis [16] one-hourly data at the nearest grid point to Hywind-Scotland have been used in this study. These data have been downloaded from the Copernicus Climate Change Service's Climate Data Store (https://cds.climate.copernicus.eu/) of European Centre of Medium Weather Forecasting (https://www.ecmwf.int/) (ECMWF) for the 1991–2020 time period, i.e. considering 30 years in order to comprehend the variations of long-term climatic patterns, as also recommended by the Worl Meteorological Organization [17]. Such data have shown very good validations for wind energy applications [23], and also for wave energy resource assessment [24].

Specifically, wind speed at 10 m height (U_{10}), wind speed at 100 m height U_{100}, peak wave period (T_p) and significant wave height (H_s) have been object of study. Additionally, the incoming direction of the wind $Udir$ and the waves $H_s dir$, by means of zonal and meridional wind speed and wave direction, have also been incorporated into the analysis. Being the focus of this paper the estimation of the energy generation and the fatigue mechanical damage of a FOWT, this was the set of variables that could be expected to have the biggest influence.

Atmospheric data from ERA5 are disseminated by default at an horizontal resolution of $0.25° \times 0.25°$, while the default grid for ocean data shows a wider resolution of $0.50° \times 0.50°$. That is why the common nearest grid point for both atmospheric and oceanic data has been selected, which is located at (−1.5°W, 57.5°N), 12 km distance from the wind farm. The exact position of the floating wind farm at the East of Scotland and the West of the North Sea is shown in Fig. 1(b).

The wind rose and the wave rose (for the zonal and meridional projections of significant wave height) diagrams for the specified location are presented, respectively, in Figs. 2(a) and 2(b), which show the main patterns of wind and wave climate in a single representation. Besides the considerable mean wind speed value at the hub height (above 9 m/s), the main characteristic of this site is the misalignment between the predominant wind direction (North) and wave direction (Southwest), consistent with the relative orientation of the coast with respect to the main wind-wave generation areas and the propagation of the waves [26]. That means, that the current analysis poses a new challenge since the directional effect of wind and waves need to be incorporated into the analysis.

Given that the hub height of the baseline NREL 5 MW wind turbine is 90 m, refer to Table 1, wind speed data at 10 m (U_{10}) and at 100 m (U_{100}) are used to compute the one-hourly roughness of the sea (z_0) using the logarithmic law that determines the vertical profile of the wind shear [27], see Eq. (1).

$$\frac{U_{100}}{U_{10}} = \frac{\log(100/z_0)}{\log(10/z_0)} \Rightarrow z_0 = e^{(((\log(2)+\log(5))(2U_{10}-U_{100}))/(U_{10}-U_{100}))} \quad [\text{m}] \tag{1}$$

By using the obtained z_0 time-series, logarithmic law can be applied again to calculate the wind speed at the hub height of the turbine (90 m) starting from U_{10}, see Eq. (2).

$$U_{90} = U_{10}\frac{\log(90/z_0)}{\log(10/z_0)} \quad [\text{m/s}] \tag{2}$$

Furthermore, wind speed data have been normalized according to the instantaneous air density computed from temperature and pressure as described in [28]. In summary, the normalization of the wind speed is given by the cubic root of the ratio between air densities, being ρ_0 the standard air density, and ρ the real air density, see Eq. (3).

$$U_{90n} = \left(\frac{\rho}{\rho_0}\right)^{\frac{1}{3}} U_{90} \quad [\text{m/s}] \tag{3}$$

2.2. Floating offshore wind turbine model

The first floating wind farm in the world is located in Hywind-Scotland and operates with a installed capacity of 30 MW, covering an area of 4 km^2 [29]. Hywind is formed by 5 equal OC3-Hywind spar-type FOWTs (see Fig. 1(a)), each with a rotor diameter of 154 m and a rated power of 6 MW. A high-fidelity model of a FOWT of very similar characteristics and using the same OC3-Hywind spar-type flotation system is available in OpenFAST [19]. Hence, this model will be used in the analysis proposed in this paper. General characteristics of the wind turbine model and the OpenFAST simulation environment employed for the aeroelastic simulations are presented in Sections 2.2.1 and 3.2, respectively.

2.2.1. Characteristics of the baseline NREL 5 MW OC3-Hywind spar-type wind turbine

The baseline NREL 5 MW wind turbine [30] with a OC3-Hywind spar-type flotation system [31] will be used in this paper for the high-fidelity evaluation of the effect of the wind and wave characteristics corresponding to a climatological normal period on the energy generation and the fatigue mechanical damage of a FOWT.

The main characteristics of the baseline NREL 5 MW wind turbine modelled in OpenFAST are presented in Table 1. Additional characteristics of the wind turbine can be found in [30].

Similarly, the main characteristics of the OC3-Hywind spar-type flotation system are shown in Table 2. Additional information about the platform and the mooring of this wind turbine are presented in [32].

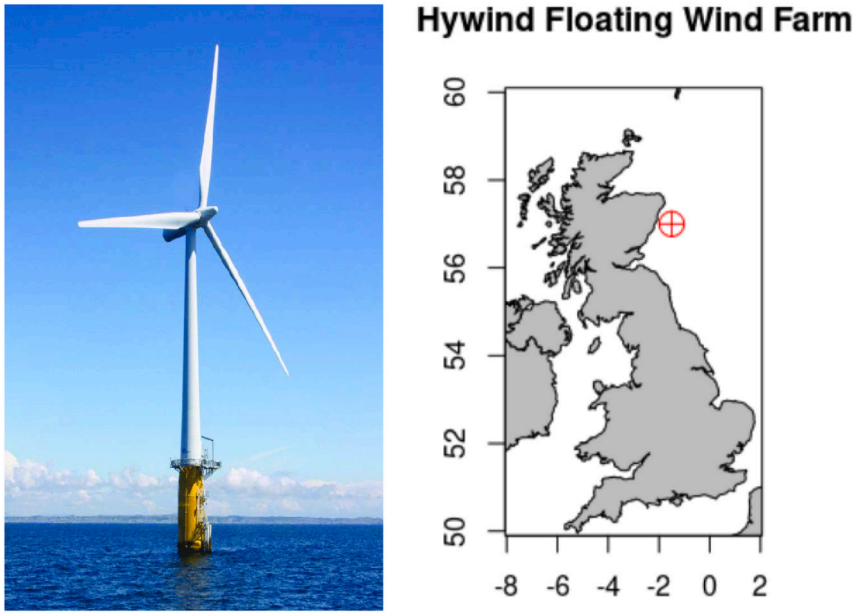

(a) (b)

Fig. 1. (a) OC3-Hywind spar-type FOWT installed in Hywind-Scotland [25]. (b) Geographical location of the Hywind-Scotland pioneering floating wind farm.

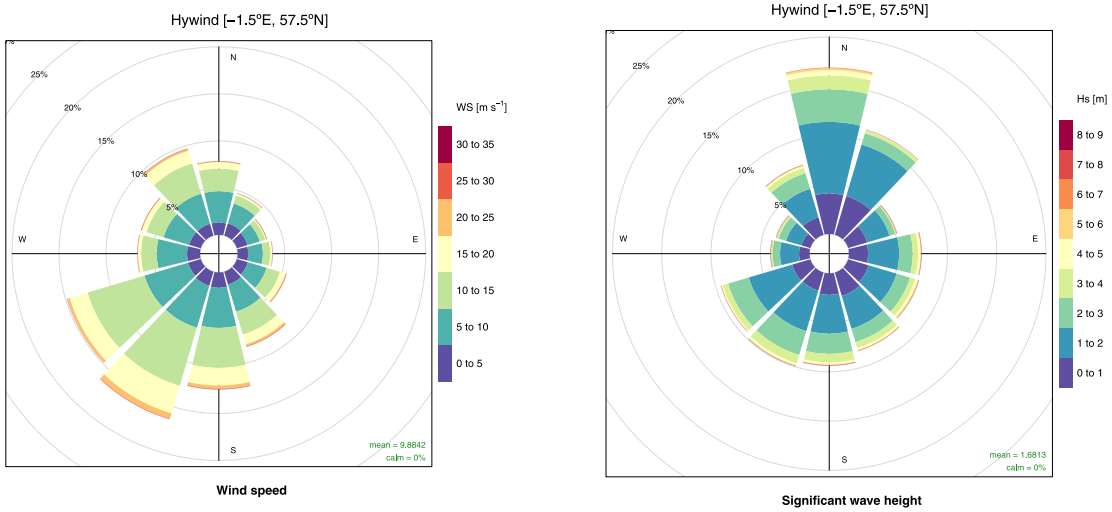

(a) Wind rose (b) Wave rose

Fig. 2. Wind and wave rose diagrams at the nearest grid point from Hywind-Scotland [−1.5°E,57.5°N].

2.2.2. OpenFAST simulation environment

OpenFAST [19] is an open-source, high-fidelity and multi-physics (includes aerodynamics, hydrodynamics for offshore structures, control and structural dynamics) aeroelastic simulation environment for the evaluation of the coupled dynamic response of a large variety of wind turbine configurations, including onshore, bottom-fixed offshore and floating offshore topologies. An overview of the various components considered in an OpenFAST simulation is presented in Fig. 3

OpenFAST v2.6.0 tool, as well as its previous releases FAST, have been widely-used in the literature for the simulation and analysis of Horizontal Axis Wind Turbines (HAWTs), both onshore and offshore, with a high degree of detail and acceptance [33]. The effect of wind-wave misalignments on the operation and mechanical loads of an offshore wind turbine is studied in [34] using FAST. Similarly, mechanical loads reduction after introduction of passive structural elements [35] or active individual pitch actuation [36] have also been analysed in the literature using this same aeroelastic code.

As part of OpenFAST simulations, the characteristics of environmental conditions, both wind and wave, can be externally defined, see Fig. 3, with respect to the scope of the conducted analysis. In this case, the objective of the present analysis is to make an assessment of the effect of wind and wave characteristics, at climatological normal period level, on the energy generation and fatigue mechanical loads of a spar-type FOWT. For that, numerous aeroelastic simulations have been conducted using different wind speed (principally defined by the mean wind speed at hub height U_{90}) and sea state (principally defined by the significant height H_s, the peak period T_p and the direction $H_s dir$ of the waves) conditions.

Turbulent wind speed fields for the simulation are generated using the stochastic turbulence emulator Turbsim [37]. As defined in the standard IEC 61400-3 [38], Kaimal spectrum, Normal Turbulence Model

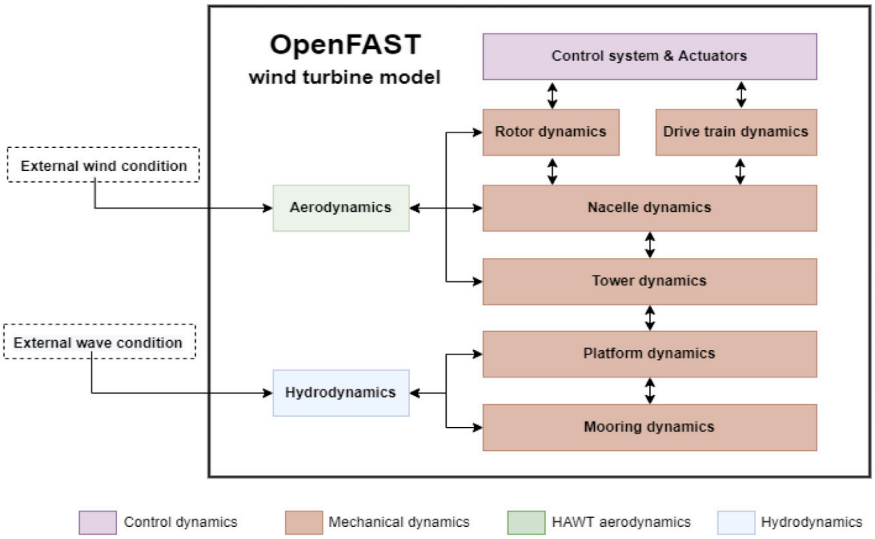

Fig. 3. Overview of the multi-physic components involved in a FOWT simulation using OpenFAST.

(NTM), and C wind class are selected for the simulation of the FOWT. In addition, irregular waves are generated based on the JONSWAP spectrum, with a peak enhancement factor calculated following the methodology in IEC 61400-3 Annex B, i.e. using peak wave period T_p and significant wave height H_s, as explained in [39].

Finally, it is to be noted that OpenFAST simulations are conducted using an external control system in Matlab-Simulink, which provides effective pitch and torque regulation to optimize the performance of the wind turbine at below rated wind speeds, limit it at beyond rated wind speeds and provide limited load reduction handles, since no additional tower damping is provided.

2.3. Methodology for power production and mechanical fatigue loads assessment

The methodology for the evaluation of the energy generation and the fatigue mechanical loads is divided into several steps, which are described in the following subsections. The characterization of the meteorological data into a reduced number of clusters is described in Section 2.3.1. The methodology to calculate power production of the FOWT is described in Section 2.3.2. Finally, the methodology to estimate the fatigue mechanical loads of the FOWT is explained in Section 2.3.3.

2.3.1. Cluster analysis of wind and sea states

As introduced in Section 1, in order to ensure computational simulation feasibility of the one-hourly observations taken during the climatological normal standard period 1991–2020, they are grouped into a reduced number of clusters. To that purpose, the Ward's minimum variance method is proposed, since it aims at finding compact, spherical clusters. This algorithm has been used in several wind studies for similar clustering purposes [22] and references therein.

Conventional similar studies are structured around the clustering of the wind [40]. While that approach might result valid for onshore wind power generation systems, additional variables are necessary to ensure reliability of an analysis of an offshore wind turbine. Due to the hydrodynamic interaction between the oceanic waves and the wind turbine, the characteristics of the wave resource will influence the operation of a FOWT and must, therefore, be included in the clustering, which increases its complexity but is required to guarantee the reliability of the results. Consequently, in this study, the hyperspace of each case is defined by the following 5 dimensions:

- U_{90} [m] wind speed at hub height.
- U_{dir} [°] incoming direction of wind.
- H_s [m] significant wave height.
- $H_s dir$ [°] incoming direction of waves.
- T_p [s] peak wave period.

After standardization of the variables, the selection of the number of clusters is made by examination of the agglomeration tree of the individual observations in the 5-D hyperspace obtained with the Ward algorithm. The distance between two cases is calculated as the square of the Euclidean distance. Going upwards in the agglomeration tree, the most similar cases (e.g those that exhibit the smallest distance among them) tend to cluster together. In Fig. 4, it can be observed, that a number of 20 clusters reasonably represents the most important groups of similar individual observations. Additionally, the wind and wave roses of the 20 clusters (not included in the paper), exhibit a clear predominant direction for most individual hourly cases belonging to those clusters.

2.3.2. Calculation of produced power

Power production of the baseline NREL 5 MW wind turbine with OC3-Hywind spar-type flotation system is evaluated considering 10 min simulations using OpenFAST framework, see Section 3.2. As specified in the standard IEC 61400-3 [38], 10 min simulations are recommended for power production scenarios. i.e. DLC 1.2 cases, considering at least 6 random seeds, thus resulting in 60 min of stochastic wind and wave inputs for each environmental condition. Plus, the low peak wave period T_p values of the sea states considered in the simulations support the use of 10 min simulations.

Therefore, the operation of the wind turbine, and especially its power production, are analysed for all 20 cluster cases obtained in Section 2.3.1. Moreover, to be consistent with the requirements in the standard IEC 61400-3, 10 different NTM wind speed seeds are simulated and post-processed for each cluster case. The inclusion of numerous seeds in the calculations reduces variability and increases robustness of the results, as it minimizes the risk of reaching conclusions based on isolated events.

Additionally, the Capacity Factor (CF) of the analysed FOWT is estimated and compared to CF values presented in related studies in the literature. A coherent CF value shall validate the environmental data considered, as well as the conducted power production calculations.

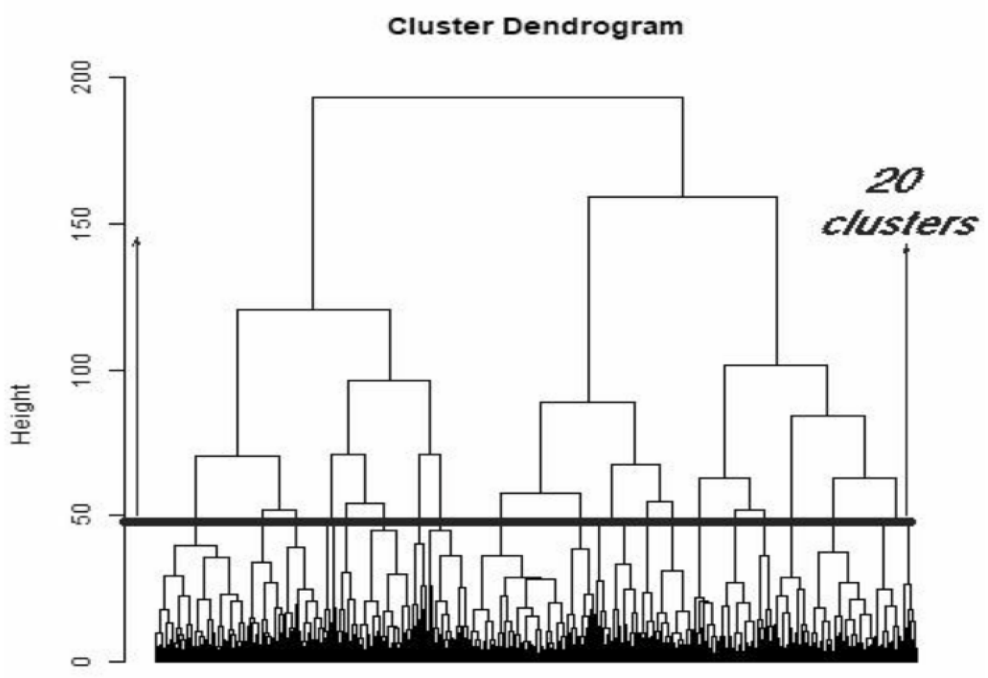

Fig. 4. Identification of clusters. Agglomeration tree obtained after execution of Ward's algorithm.

2.3.3. Estimation of fatigue mechanical loads

The estimation of the fatigue mechanical damage in the main components of the wind turbine is accomplished by post-processing of OpenFAST simulation results using software tool MLife [41]. The application of this tool for the calculation of fatigue mechanical loads associated to active control strategies in a HAWT [42] or to determine mechanical short-term affection of oceanic waves in the tower of a FOWT [43] can be found in the literature.

Fatigue damage estimation is fundamentally based on the calculation of mechanical loads in the time domain, the application of a rainflow counting algorithm to determine the number of cycles and a latter cumulative damage calculation based on the S-N curve corresponding to the material of the mechanical component [44]. In this case, as it is presented in Fig. 5, the mechanical loads in the time domain are obtained through simulation of DLC 1.2 cases considering the 20 clusters obtained in Section 2.3.1 and using OpenFAST framework, see Section 3.2. Again, according to the standard IEC 61400-3, the length of the simulation has been set to 10 min and 10 different NTM wind speed seeds are simulated and post-processed, in order to reduce variability of the obtained results.

The list of mechanical bending moment elements selected for fatigue post-processing, as well as a brief description of each of them, is presented in Table 3. These elements are a reflection of the most important mechanical moments in the core components of a HAWT, i.e. tower, LSS and blades, and shall therefore be used as performance indicators of the main subsystems in a HAWT. Same performance indicators are used in similar mechanical fatigue loads estimation studies in the literature [45].

Material exponents m selected for the calculation of the fatigue damage (in a time horizon of 30 years) are 3,4,5 for the tower and the LSS and 8,10,12 for the blades. This selection responds to the material of each component, steel for the tower and the LSS and composite for the blades [45].

Finally, MLife weights the fatigue Damage Equivalent Load (DEL) of each bending moment element by the statistical terms given by the Weibull distribution and its characteristic parameters, scale k and form c, which determine the frequency of occurrence of each wind speed bin interval [27]. In case of onshore wind turbines, the probability of occurrence of the wind might suffice for the long-term fatigue damage calculation. Nevertheless, for offshore wind turbines, the statistical distribution of the sea states must also be considered in order to achieve reliable results.

Table 3
List of bending moment elements selected for fatigue post-processing, named after their abbreviations in OpenFAST.

Name	Description	Unit
RootMxb1	Edgewise bending moment at the blade root	[kN m]
RootMyb1	Flapwise bending moment at the blade root	[kN m]
RootMzb1	Pitch bending moment at the blade root	[kN m]
RotTorq	Rotor torque, constant along the LSS	[kN m]
LSSGagMya	Rotating y-axis bending moment at the LSS strain gage	[kN m]
LSSGagMza	Rotating z-axis bending moment at the LSS strain gage	[kN m]
TwrBsMxt	Side-side (or roll) bending moment at the tower base	[kN m]
TwrBsMyt	Fore-aft (or pitch) bending moment at the tower base	[kN m]
TwrBsMzt	Torsional (or yaw) bending moment at the tower base	[kN m]

On account of the restrictions to consider the statistical distribution of the sea states in the MLife post-processing, the fatigue DEL calculation is done in two steps. For that, the probability of occurrence of each cluster wind speed P_U is computed considering the 95% confidence interval of its centroid, i.e. $U_{90}\epsilon\ [U_{90,q05}, U_{90,q95}]$, as it is shown in Eq. (4).

$$P_{U,i} = e^{-(\frac{U_{q05,i}}{c})^k} - e^{-(\frac{U_{q95,i}}{c})^k} \tag{4}$$

where N refers to the total number of clusters and $i\epsilon\{1,\ldots,N\}$.

In the first step, the scale and form factors are defined with their standard value, $k = 2$ and $c = 6$ m/s, and the standard probability of occurrence P_{st} is calculated. However, the real statistical contribution of each cluster i is provided by its probability of occurrence P_c, which is shown in the last column in Table 4. Therefore, the original fatigue DEL values provided by MLife are normalized by P_{st} and re-weighted by P_c, which already considers the statistical distribution of U_{90}, U_{dir}, H_s, $H_s dir$ and T_p for each cluster. This procedure gives the final fatigue DEL value by the pondered contributions of all clusters, see Eq. (5).

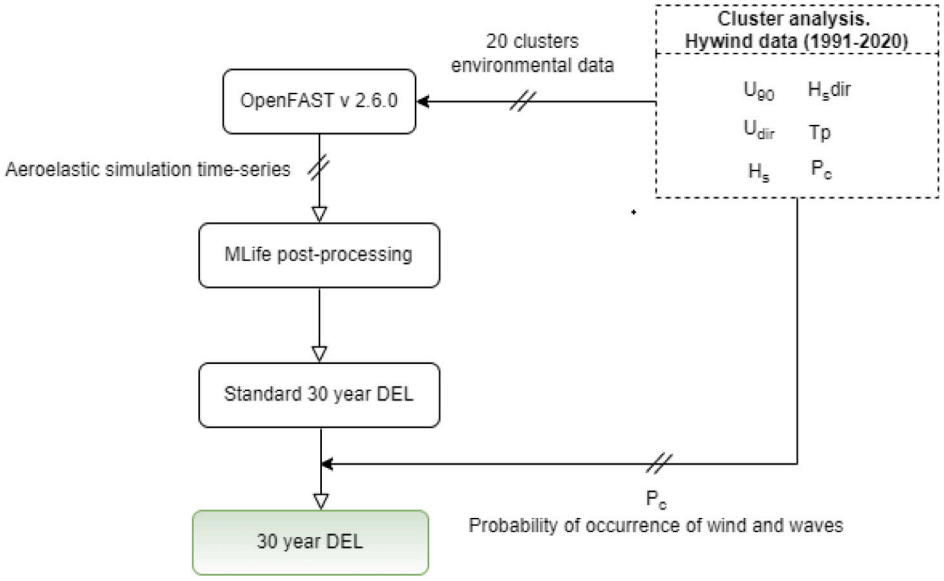

Fig. 5. Schematic diagram of the procedure for the estimation of the fatigue mechanical damage of the FOWT.

$$DEL_f = \sum_{i=1}^{N} DEL_i \frac{P_{c,i}}{P_{st,i}} \quad (5)$$

where N refers to the total number of clusters and $i \epsilon \{1, \ldots, N\}$.

3. Results

The results of the cluster analysis and the subsequent characterization of the meteorological data into a reduced number of cases is described in Section 3.1. Section 3.2 shows the results related to the evaluation of the power and energy production of the FOWT. Finally, results corresponding to the estimation of the fatigue mechanical loads are presented in Section 3.3.

3.1. Identification of cluster classes

The centroids of the clusters described in Section 2.3.1 can be considered as the major wind-sea combined state-types in which all the observations in the area for the analysed 30 years period can be grouped. The list of 20 cluster classes obtained after execution of the clustering process using Ward's minimum variance method is presented in Table 4. All hourly climate observations in the analysed 30 years exhibit the smallest distance to one of this particular centroids or, in other words, belong to one of the clusters.

As representatives of the major wind-sea combinations in Hywind-Scotland for the last climatological normal standard period (30 years, 1991–2020), the environmental conditions defined by the clusters in Table 4 are simulated using the aeroelastic code OpenFAST v2.6.0 in order to evaluate in detail the power production and fatigue mechanical loads (with the same time horizon of 30 years) of a FOWT in such environmental conditions.

The last column in Table 4 represents the probability of occurrence of the cluster during the analysed 1991–2020 period. This probability must be considered in the estimation of the fatigue mechanical damage, in order to successfully match each set of environmental conditions to their actual occurrence, and compute long-term damage in a realistic way.

3.2. Evaluation of power and energy production

As described in Section 2.3.2, the evaluation of the power production of the FOWT is based on the simulation of DLC 1.2 cases, with a simulation time of 600 s. After that, the produced power and general operation variables of the FOWT at all set of environmental conditions defined in 3.1 can be analysed. Additionally, in order to assess the effect of the waves on the operation and power production of the wind turbine, the operation of the same FOWT have been simulated at still water state, but considering the same wind condition of each cluster. Note that for all 20 clusters 10 different turbulent wind speed seeds have been simulated, in order to reduce variability of the results and increase robustness of the conclusions.

The negligible affection of the waves on the power production and overall operation of the FOWT is shown in Fig. 6. For that, the following simulation cases are shown:

- Wind conditions in cluster 1, turbulent seed 1 and still water (straight blue line).
- Wind and wave conditions in cluster 1, turbulent seed 1 (dashed yellow line).
- Wind conditions in cluster 1, turbulent seed 3 and still water (straight purple line).

Table 4
Cluster centroids and percentage of occurrence.

Cluster #	U_{90} [m/s]	U_{dir} [°]	H_s [m]	$H_s dir$ [°]	T_p [s]	P_c [% of occurrence]
1	11.2	119.8	2.2	93	7.8	6.6
2	14.9	169.6	2.3	161.1	6.5	7.1
3	6	92	1.1	167.4	8.6	0.3
4	8	181.7	0.8	153.6	4.8	10.6
5	11.9	189.1	2.7	120.3	8.8	1.4
6	7.9	249.4	0.9	254.3	4.8	4.8
7	4.7	184.8	1	97.1	8.6	10.1
8	8.7	205.1	1.4	172.8	11.5	1.1
9	13.8	223.2	2.3	187.5	6.9	4.7
10	13.8	232.2	2.1	230.5	5.9	14.5
11	7.7	232.7	1	135.9	5.9	0.98
12	10.4	225.1	1.9	54.8	8.6	0.04
13	14	252.9	2.8	297	8.1	0.3
14	12	317.6	2.2	285.6	7	9.7
15	6	125	0.9	96.4	5.5	9.6
16	12.5	200	2.9	57.4	9.4	4.5
17	7	304.1	1.2	153.2	6.5	1.4
18	14.7	300.2	3	225	8.3	0.1
19	8.7	82.2	2.2	85.2	8.5	2.6
20	7.1	241.6	1.7	192.7	11.3	9.5

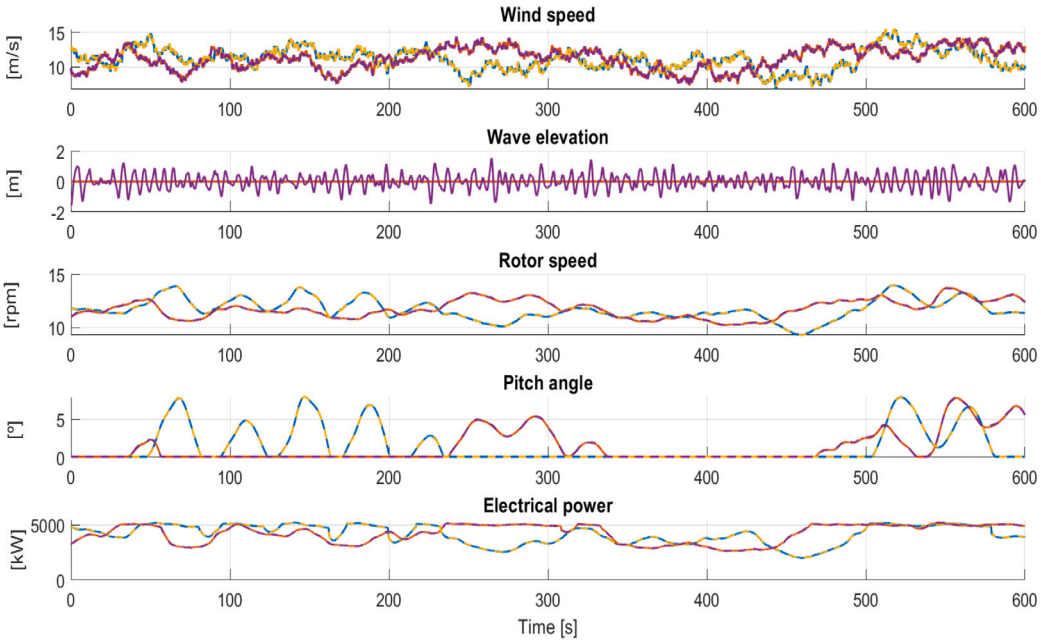

Fig. 6. OpenFAST based time-domain operation and power production of the FOWT in various environmental conditions.

- Wind and wave conditions in cluster 1, turbulent seed 3 (dashed orange line).

Besides wind speed and instantaneous wave elevation, rotor speed, pitch angle and electrical power are analysed as major representatives of the operation of the wind turbine. While electrical power production is usually the final and most-widely analysed concept, as it defines Annual Energy Production (AEP), rotor speed and pitch angle are necessary to evaluate the correct operation of the wind turbine and interpret the instantaneous electrical power production value.

The simulation results show that the operation of the wind turbine is not remarkably altered by the interaction with the waves, as there is no obvious difference in any of the operational variables, including electrical power production. In addition, the conclusion is valid for both turbulent wind speed seeds that have been represented in Fig. 6, which infers that it is not an isolated coincidence.

However, in order to demonstrate the general validity of the conclusions, the deviation (in [%]) between the electrical power production in case of still water and in case of interaction with waves is represented in Fig. 7, for each cluster and each turbulent wind speed seed. Finally, the statistical mean deviation value for each one of the clusters is calculated and represented using the dashed black line.

It is to be observed that the mean deviation in the electrical power production does not exceed 0.2% in any of the clusters, which might even be affected by simulation uncertainties of the aeroelastic code OpenFAST. Hence, in light of the lack of a pattern that explains a systematical power loss due to the interaction of the FOWT with the waves, it can be concluded that there will be no effect of Hywind-Scotland waves on the AEP of the FOWTs.

Therefore, conventional Weibull distribution based calculations can be used for the estimation of the energy generation of a FOWT installed in Hywind-Scotland wind farm and during the studied climate period (1991–2020). Those calculations can be summarized as a fitting of the scale and form (k and c) parameters related to the Weibull distribution to match the 30 year wind speed data, and a latter implementation of the power curve of the FOWT on the fitted histogram to estimate its energy production. Note that, in this case, the power curve of the FOWT has been calculated using the same simulation environment described in Section 2.2.2 and considering 10 different turbulent wind speed seeds to reduce variability. The results of the fitting procedure on the histogram (the values of the Weibull parameters), the AEP and the corresponding CF are shown in Fig. 8.

3.3. Estimation of fatigue mechanical loads

In addition to the power production of the FOWT, the fatigue mechanical damage in its main components have also been calculated and evaluated. In contrast to the electrical power production, which have been observed to remain invariable, the fatigue damage in some of the mechanical components of the wind turbine, especially the tower, is expected to increase as a result of the hydrodynamic interaction with the oceanic waves.

As described in Section 2.3.3, DLC 1.2 cases, with a simulation time of 600 s, have simulated to calculate the time-domain mechanical loads necessary for the estimation of the fatigue damage of the main mechanical components of the wind turbine. Additionally, in order to assess the effect of the waves on the fatigue damage of the wind turbine, the operation of the same FOWT have been simulated at still water state, but considering the same wind condition of each cluster. Again, note that for all 20 clusters 10 different turbulent wind speed seeds have been simulated, in order to reduce variability of the results and increase robustness of the conclusions.

A preliminary analysis of the expected fatigue mechanical damage on the wind turbine components can be performed using the time-domain bending moments presented in Fig. 9. For that, the following simulation cases are shown:

- Wind conditions in cluster 1, turbulent seed 1 and still water (orange line).
- Wind and wave conditions in cluster 1, turbulent seed 1 (blue line).

It is to be observed in Fig. 9 that the tower side-side is the most heavily affected bending moment due to the hydrodynamic excitation exerted by the oceanic waves. In fact, the affection of the waves on the blade edgewise bending moment and the rotor torque is limited, as no integral differences between the simulations with still water and waves are detected. Thus, the expectation is to notice remarkable fatigue damage increment principally in the tower base bending moment elements.

The equivalent fatigue DELs through the climatological period 1991–2020, for both still water and wave conditions, are presented in Table 5.

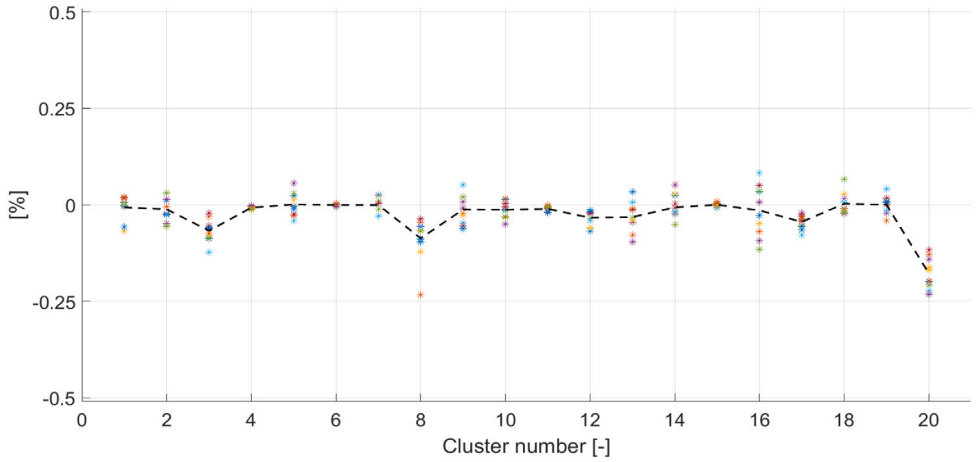

Fig. 7. Deviation (in [%]) between the electrical power production of the FOWT in case of still water and considering the waves.

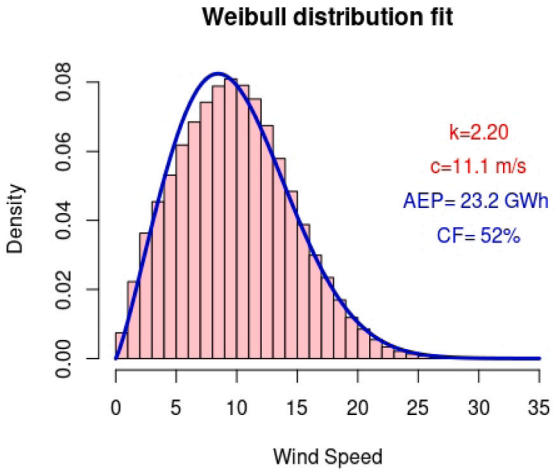

Fig. 8. Weibull fitting and estimated energy production of a FOWT in Hywind-Scotland during the time period 1991–2020.

Furthermore, in order to facilitate the comparison and the evaluation of the affection of the oceanic waves on the fatigue damage of each one of the components, the relative increments (in [%]) of each bending moment are presented in Table 6.

The largest relative increment values in Table 6 are highlighted in red, the intensity of the colour being proportional to the value of the increment. The results support the expected premises, as the main increments are observed in the tower side-side and fore-aft bending moments, which was to be expected after the preliminary analysis of the time-domain bending moments presented in Fig. 9. The relative increment of the DEL of the rest of the bending moments is negligible, as such small values could even be considered to be due to simulation uncertainties.

Fatigue mechanical loads are heavily dependent on the characteristics of the wind turbine, the environmental conditions and the DLCs considered. Therefore, even though the obtained results are hardly comparable in absence of certainty of identical conditions having been considered in the input data, the similar DEL values presented in [46] in calculations with the same wind turbine shall serve for the validation of the presented results. Other studies in which quadrature rule techniques are applied to the fatigue load calculations [47] also presented consistent although not identical results.

Table 5
30 year equivalent fatigue mechanical DELs ([kN m]). Still water in black and waves consideration in blue.

	30 year fatigue DELs [kN m]. Still water \			Waves		
	3	4	5	8	10	12
RootMxb1				3115.61 3119.18	3265.20 3267.48	3376.46 3377.07
RootMyb1				2455.86 2463.14	2762.41 2775.85	3009.19 3020.05
RootMzb1				49.31 49.52	53.71 53.95	57.20 57.49
RotTorq	208.85 210.14	278.45 279.92	346.07 347.38			
LSSGagMya	1679.93 1681.39	1986.60 1990.51	2232.31 2235.15			
LSSGagMza	1678.62 1678.63	1985.89 1986.65	2225.21 2224.72			
TwrBsMxt	2477.95 6151.60	3029.79 7542.50	3542.40 8682.42			
TwrBsMyt	12 651.56 13 675.49	16 961.72 18 281.12	20 561.73 22 114.09			
TwrBsMzt	985.59 986.43	1135.88 1141.13	1294.02 1298.43			

Table 6
Relative increment (in [%]) of fatigue mechanical DELs due to hydrodynamic interaction of the FOWT with the oceanic waves.

	Comparison of 30 year fatigue DELs [%]					
	3	4	5	8	10	12
RootMxb1				0.11	0.07	0.02
RootMyb1				0.30	0.49	0.36
RootMzb1				0.44	0.45	0.51
RotTorq	0.61	0.53	0.38			
LSSGagMya	0.09	0.20	0.13			
LSSGagMza	0.00	0.04	-0.02			
TwrBsMxt	148.25	148.94	145.10			
TwrBsMyt	8.09	7.78	7.55			
TwrBsMzt	0.08	0.46	0.34			

4. Discussion

The methodology presented in this paper reduces the computational cost and simplifies the estimation process of energy production and fatigue mechanical damage for FOWTs, even though the complexity of the problem is incremented by introducing new ocean-related variables, such as wave height, period and direction, which are unaccountable in case of onshore wind turbines. This is accomplished by execution

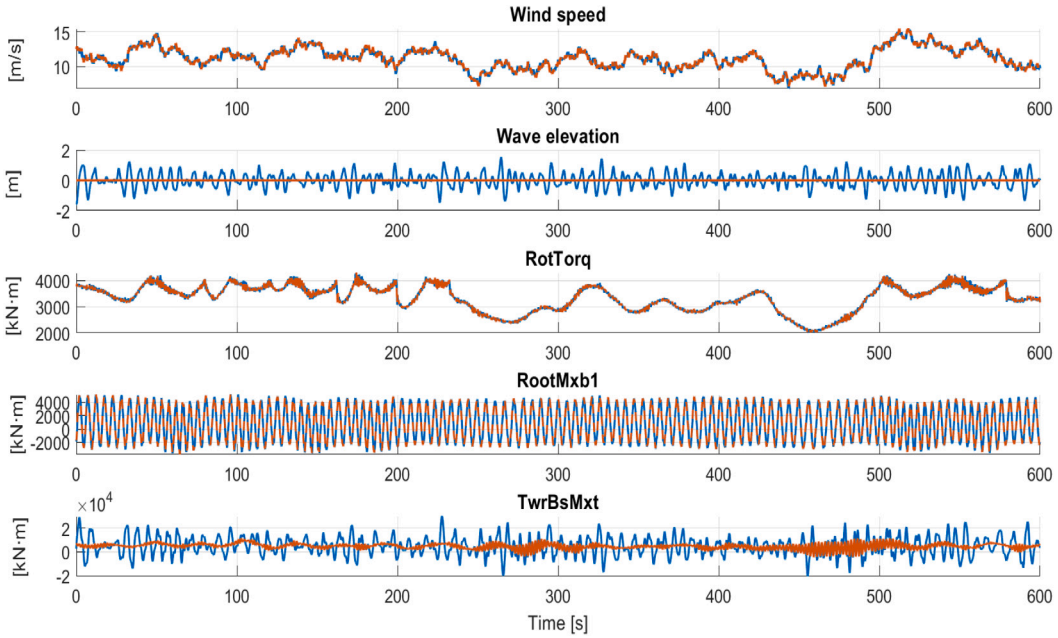

Fig. 9. OpenFAST based time-domain mechanical bending moments of the FOWT in various environmental conditions.

of a cluster classification. Whereas the presented results are specific for the characteristics of the baseline NREL 5 MW wind turbine with OC3-Hywind spar-type floating system, a general methodology is established, which can therefore be applied for any other FOWT with different characteristics. In this case, although the number of potential load cases to simulate might be infinite, the presented analysis is based on the simulation and post-processing of load cases in which the FOWT produces power in standard environmental conditions, as they are considered to be the harshest in terms of mechanical loading, supported by their probability of occurrence in a 30 years time horizon.

In regards to the power production analysis of the FOWT, and the subsequent energy generation, it is demonstrated that the influence of the predominant wave conditions on the efficiency of the offshore wind farm can be attenuated by the design of an adequate SW based regulation of the turbine. This regulation should avoid interactions between control dynamics and mechanical oscillations caused by the waves, allowing the operation of the wind turbine to remain invariable with respect to the waves. Even though this conclusion supports the installation of future floating offshore wind farms, it must be noted that, prior to the installation of these FOWTs, the load analysis presented in this paper should be extended to incorporate extreme events. In this case, the analysis has been limited to the predominant environmental conditions, and the consequent fatigue mechanical damage. However, the well-being of the turbine facing extreme sea states must also be ensured.

The invariability of the power production of the FOWTs with respect to the predominant wave conditions also allows a fundamental decoupling between the estimation of the energy generation by a FOWT and the sea states, limiting the variables necessary to be considered in the estimation process and, therefore, simplifying it. The obtained value of CF 52% is coherent with this premise, as it presents the same value as similar studies in the literature for offshore wind farms and for the last news on annual energy production records at Hywind [48].

Regarding fatigue mechanical damage in the main components of the FOWTs, a considerable increment of the side-side bending moment of the tower has been noticed as a result of the hydrodynamic interaction of the structure of the wind turbine with the oceanic waves. A milder increase of the fore-aft bending moment of the tower has also been detected. The estimation of this DEL increments is important, since it must be considered during the design process of the wind turbine, in order to account for the mechanical loads the FOWT needs to withstand during its lifetime. Note that as consequence of the thrust force, which actuates in the same direction as the rotor orientation, the absolute value of the fore-aft bending moment is still much larger than the incremented side-side bending moment. The fatigue damage increment due to the sideways propagating waves can therefore be better understood.

In this context, Hywind-Scotland constitutes a paradigmatic location due to the misalignment of the predominant direction of the wind and the propagation of the waves, as it is shown in the wind rose (Fig. 2(a)) and the wave rose (Fig. 2(b)). For instance, it is well known that the North-Westerns swell and winds that govern the sea states in the Irish, Portuguese or Gulf of Biscay's shoreline would cause even higher increments of the DEL in the fore-aft bending moment. On the contrary, the strong Western component of the waves relative to the predominant Northern winds at Hywind, generate the particular increment of loads for the side-side bending moment, as it is shown in Table 6.

In general, the reduced increment of the fatigue mechanical DELs in the rest of the mechanical components of the FOWT, lessens the potential consequences of installing floating wind farms. However, before generalizing the conclusion, the analysis should be broadened to other FOWT designs, as there could be increased loads due to the different mechanical properties of a different FOWT. The use of the IEA Wind 15-Megawatt Offshore Reference Wind Turbine [49] is expected in future analyses.

The methodology proposed in this paper could serve for various purposes. On the one hand, the long-term fatigue damage of existing offshore wind turbines could be estimated based on the environmental data since the installation of the wind turbines. In fact, due to the nature of the proposed methodology, large amounts of data can be reduced into a computationally affordable number of cases, including their probability of occurrence, and long periods of time can be analysed. However, in future analyses this methodology could also be used for the selection of optimal wind farm locations based on not only past, but also future meteorological conditions in different Shared Socioeconomic Pathway (SSP) scenarios of CMIP6 [50]. Past data shall detect environmental patterns in the potential locations that support the installation of the wind farm, while future projections can be used to estimate the energy generation and fatigue mechanical damage of a wind turbine in that location after its installation. The combination

of both features might optimize the location selection procedure in a context of climate oscillations, where this approach could be applied to estimate future energy production, fatigue loads and economical feasibility of wind farms now being put into operation. The centroids represent the characteristic combined wind-sea states whose frequency of occurrence may change in the future like in other areas such as the Bay of Biscay [51] or other regions worldwide such as the regions affected by the trade winds, to name another example [52].

Finally, this methodology could also be used for pure investigative purposes in which the effects of climate change patterns in the behaviour and maintenance of wind turbines could be analysed, e.g. within the context of increment of extreme ocean events because of global warming [53].

In the future, the hydrodynamics of the proposed method can be improved using new open-source alternatives. Evaluation of the ocean wave load is conventionally done by commercial software, such as WAMIT. However, in recent years some newly developed open-source free software has become available for this purpose. In Oct. 2020, an open-source offshore hydrodynamics code—HAMS was released publicly to the field of ocean renewable energy [54], including floating wind energy [55] and wave energy [56]. Wave loads acting on the floating foundation of a floating wind turbine (spar, semi-submersible, TLP, etc.) can be computed against the wave climates at a specific local site, such as wave incident angle, wave height, wave frequency and water depth. HAMS can generate the hydrodynamic force coefficients required by OpenFAST and can be used with a visual user interface BEMRosetta [57] which can view the output channels from OpenFAST. In addition, a new open-source tool RAFT [58] for floating wind turbine optimization is developed by NREL using HAMS as the hydrodynamic basis.

5. Conclusions

A new methodology for the long-term estimation of the energy generation and fatigue mechanical damage of FOWTs is presented in this paper, combining cluster analysis for wind and wave data, statistical distribution of the environmental data, and their effect in a high-detailed aeroelastic wind turbine model, i.e. OpenFAST. A time horizon of 30 years has been selected for the energy and fatigue estimation, in order to consider the variability of the climatic patterns and have a consistent approximation:

- This methodology can be coherently projected for future 30 year periods, generating a new way for long-term operation and maintenance prediction based on expected fatigues, which nowadays constitutes one of the mayor challenges of offshore renewable energy extraction.
- Results show that there is limited affection of the waves to the operation and power production of a FOWT. Hence, the energy generation of the turbines might be considered unrelated to the predominant sea states in the Hywind-Scotland locations and the estimation process of the energy is simplified, as a reduced number of environmental conditions can be considered.
- On the other hand, a substantial increment of the long-term fatigue DEL in the tower side-side and fore-aft bending moments have been detected, especially the former, as almost a 150% increment has been estimated. Such increments should be considered during the design of the wind turbine, if premature failures of the wind turbine are to be avoided. The affection is negligible on the rest of the analysed mechanical components.
- It must be noted that the obtained conclusions are limited to the scope of this study, i.e. the specific characteristics of the baseline NREL 5 MW wind turbine with OC3-Hywind spar-type and the dominant sea states in the Hywind-Scotland location. Therefore, the conclusions should not be generalized to all wind turbine configurations. Likewise, extreme environmental conditions have been considered to be beyond the scope of the paper.
- Finally, this methodology could be used not only for the estimation of energy generation and fatigue damage in already installed wind turbines, but also for the selection of optimal wind farm locations based on past data and future meteorological projections, as well as the study of climate change patterns on the energy generation and fatigue damage of FOWTs.

CRediT authorship contribution statement

Aitor Saenz-Aguirre: Conceptualization, Investigation, Methodology, Software, Writing – original draft, Writing – review & editing. **Alain Ulazia:** Conceptualization, Investigation, Methodology, Software, Writing – original draft. **Gabriel Ibarra-Berastegi:** Methodology, Software, Supervision, Writing – review & editing. **Jon Saenz:** Supervision, Writing – original draft.

Declaration of competing interest

The authors declare that they have no known competing financial interests or personal relationships that could have appeared to influence the work reported in this paper.

Data availability

Data will be made available on request.

Acknowledgements

The authors acknowledge grant PID2020-116153RB-I00 funded by MCIN/AEI/10.13039/501100011033 and, as appropriate, by "ERDF A way of making Europe", by the "European Union" or by the "European Union NextGenerationEU/PRTR". Additionally, financial support by the University of the Basque Country under the contract (UPV/EHU project GIU20/008) has been received.

References

[1] Bilgili M, Yasar A, Simsek E. Offshore wind power development in Europe and its comparison with onshore counterpart. Renew Sustain Energy Rev 2011;15(2):905–15.
[2] EWEA-wind Europe (European wind energy association). Key trends and statistics; EWEA. Tech. rep., Brussels, Belgium: EWEA; 2017.
[3] Robertson B, Dunkle G, Gadasi J, Garcia-Medina G, Yang Z. Holistic marine energy resource assessments: A wave and offshore wind perspective of metocean conditions. Renew Energy 2021;170:286–301.
[4] Offshore wind energy (OWE). Technology of OWE; 2009, http://Www.Offshorewindenergy.org/.
[5] Martinez A, Iglesias G. Multi-parameter analysis and mapping of the levelised cost of energy from floating offshore wind in the Mediterranean Sea. Energy Convers Manage 2021;243:114416.
[6] Carballo R, Sánchez M, Ramos V, Fraguela J, Iglesias G. Intra-annual wave resource characterization for energy exploitation: A new decision-aid tool. Energy Convers Manage 2015;93:1–8.
[7] Weinzettel J, Reenaas M, Solli C, Hertwich EG. Life cycle assessment of a floating offshore wind turbine. Renew Energy 2009;34(3):742–7.
[8] Jungbluth N, Bauer C, Dones R, Frischknecht R. Life cycle assessment for emerging technologies: case studies for photovoltaic and wind power (11 pp). Int. J. Life Cycle Assess. 2005;10(1):24–34.
[9] Cheng P, Huang Y, Wan D. A numerical model for fully coupled aero-hydrodynamic analysis of floating offshore wind turbine. Ocean Eng 2019;173:183–96.
[10] Salic T, Charpentier JF, Benbouzid M, Le Boulluec M. Control strategies for floating offshore wind turbine: Challenges and trends. Electronics 2019;8(10):1185.
[11] Lackner MA. Controlling platform motions and reducing blade loads for floating wind turbines. Wind Eng. 2009;33(6):541–53.
[12] Li X, Gao H. Load mitigation for a floating wind turbine via generalized H_∞ structural control. IEEE Trans Ind Electron 2015;63(1):332–42.
[13] Veigas M, Iglesias G. Wave and offshore wind potential for the island of tenerife. Energy Convers Manage 2013;76:738–45.
[14] Saenz-Aguirre A, Saenz J, Ulazia A, Ibarra-Berastegui G. Optimal strategies of deployment of far offshore co-located wind-wave energy farms. Energy Convers Manage 2022;251:114914.

[15] Astariz S, Perez-Collazo C, Abanades J, Iglesias G. Co-located wind-wave farm synergies (Operation & Maintenance): A case study. Energy Convers Manage 2015;91:63–75.

[16] Hersbach H, Bell B, Berrisford P, Hirahara S, Horányi A, Muñoz-Sabater J, Nicolas J, Peubey C, Radu R, Schepers D, et al. The ERA5 global reanalysis. Q J R Meteorol Soc 2020;146(730):1999–2049.

[17] WMO guidelines on the calculation of climate normals. Tech. rep. WMO-No. 1203, Geneva, Switzerland: World Meteorological Organization; 2017, p. 18.

[18] Changing the reference period from 1981–2020 to 1991–2020 for the C3S climate bulletin. 2021, URL https://climate.copernicus.eu/sites/default/files/2021-02/C3S_Climate_Bulletin_change_from_1981-2010_to_1991-2020_reference_period_v08-Feb-20_all.pdf.

[19] Openfast v3.1.0. 2022, available at https://github.com/OpenFAST/openfast (Accessed on 20 May 2022).

[20] Saenz-Aguirre A, Fernandez-Gamiz U, Zulueta E, Aramendia I, Teso-Fz-Betono D. Flow control based 5 MW wind turbine enhanced energy production for hydrogen generation cost reduction. Int J Hydrogen Energy 2020.

[21] Yang Y, Bashir M, Wang J, Yu J, Li C. Performance evaluation of an integrated floating energy system based on coupled analysis. Energy Convers Manage 2020;223:113308.

[22] Babaei M, Azizi E, Beheshti MT, Hadian M. Data-driven load management of stand-alone residential buildings including renewable resources, energy storage system, and electric vehicle. J Energy Storage 2020;28:101221. http://dx.doi.org/10.1016/j.est.2020.101221, URL https://www.sciencedirect.com/science/article/pii/S2352152X19306383.

[23] Sreelakshmi S, Bhaskaran PK. Wind-generated wave climate variability in the Indian Ocean using ERA-5 dataset. Ocean Eng 2020;209:107486.

[24] Ulazia A, Esnaola G, Serras P, Penalba M. On the impact of long-term wave trends on the geometry optimisation of oscillating water column wave energy converters. Energy 2020;206:118146.

[25] Driscoll F, Jonkman J, Robertson A, Sirnivas S, Skaare B, Nielsen FG. Validation of a FAST model of the statoil-hywind demo floating wind turbine. Energy Procedia 2016;94(NREL/JA-5000-66650).

[26] Passaro M, Hemer MA, Quartly GD, Schwatke C, Dettmering D, Seitz F. Global coastal attenuation of wind-waves observed with radar altimetry. Nature Commun 2021;12:3812. http://dx.doi.org/10.1038/s41467-021-23982-4.

[27] Manwell JF, McGowan JG, Rogers AL. Wind energy explained: theory, design and application. John Wiley & Sons; 2010.

[28] Ulazia A, Ibarra-Berastegi G, Sáenz J, Carreno-Madinabeitia S, González-Rojí SJ. Seasonal correction of offshore wind energy potential due to air density: Case of the iberian peninsula. Sustainability 2019;11(13):3648.

[29] https://www.equinor.com/energy/hywind-scotland (Accessed on 20 May 2022).

[30] Jonkman J, Butterfield S, Musial W, Scott G. Definition of a 5-MW reference wind turbine for offshore system development. Tech. rep., Golden, CO (United States): National Renewable Energy Lab.(NREL); 2009.

[31] Jonkman J. Definition of the floating system for phase IV of OC3. Tech. rep., Golden, CO (United States): National Renewable Energy Lab.(NREL); 2010.

[32] Xu X, Srinil N. Dynamic response analysis of spar-type floating wind turbines and mooring lines with uncoupled vs coupled models. In: International conference on offshore mechanics and arctic engineering, Vol. 56574. American Society of Mechanical Engineers; 2015, V009T09A062.

[33] Golparvar B, Papadopoulos P, Ezzat AA, Wang R-Q. A surrogate-model-based approach for estimating the first and second-order moments of offshore wind power. Appl Energy 2021;299:117286.

[34] Stewart GM, Lackner MA. The impact of passive tuned mass dampers and wind–wave misalignment on offshore wind turbine loads. Eng Struct 2014;73:54–61.

[35] Lackner MA, Rotea MA. Passive structural control of offshore wind turbines. Wind Energy 2011;14(3):373–88.

[36] Namik H, Stol K. Individual blade pitch control of floating offshore wind turbines. Wind Energy: Int J Prog Appl Wind Power Convers Technol 2010;13(1):74–85.

[37] Jonkman BJ. TurbSim user's guide. Tech. rep., Golden, CO (United States): National Renewable Energy Lab.(NREL); 2006.

[38] Commission IE, et al. Wind energy generation systems-part 3-2: design requirements for floating offshore wind turbines. Geneva, Switzerland: IEC TS; 2019, p. 61400–3.

[39] Saenz-Aguirre A, Ulazia A, Ibarra-Berastegui G, Saenz J. Extension and improvement of synchronous linear generator based point absorber operation in high wave excitation scenarios. Ocean Eng 2021;239:109844.

[40] AZIZI E, KHARRATI-SHISHAVAN H, MOHAMMADI-IVATLOO B, SHOTORBANI AM. Wind speed clustering using linkage-ward method: A case study of khaaf, iran. Gazi Univ J Sci 2019;32(3):945–54.

[41] Hayman G. MLife theory manual for version 1.00, Vol. 74. Golden, CO: National Renewable Energy Laboratory; 2012, p. 106, (75).

[42] Yuan Y, Tang J. Adaptive pitch control of wind turbine for load mitigation under structural uncertainties. Renew Energy 2017;105:483–94.

[43] Li H, Hu Z, Wang J, Meng X. Short-term fatigue analysis for tower base of a spar-type wind turbine under stochastic wind-wave loads. International Journal of Naval Architecture and Ocean Engineering 2018;10(1):9–20.

[44] Kvittem MI, Moan T. Time domain analysis procedures for fatigue assessment of a semi-submersible wind turbine. Mar Struct 2015;40:38–59.

[45] Haid L, Stewart G, Jonkman J, Robertson A, Lackner M, Matha D. Simulation-length requirements in the loads analysis of offshore floating wind turbines. In: International conference on offshore mechanics and arctic engineering, Vol. 55423. American Society of Mechanical Engineers; 2013, V008T09A091.

[46] Matha D. Model development and loads analysis of an offshore wind turbine on a tension leg platform with a comparison to other floating turbine concepts: April 2009. Tech. rep., Golden, CO (United States): National Renewable Energy Lab.(NREL); 2010.

[47] van den Bos L, Bierbooms W, Alexandre A, Sanderse B, van Bussel G. Fatigue design load calculations of the offshore NREL 5 MW benchmark turbine using quadrature rule techniques. Wind Energy 2020;23(5):1181–95.

[48] EQUINOR. Hywind Scotland remains the UK's best performing offshore wind farm. 2021, URL.

[49] Gaertner E, Rinker J, Sethuraman L, Zahle F, Anderson B, Barter GE, Abbas NJ, Meng F, Bortolotti P, Skrzypinski W, et al. IEA wind TCP task 37: definition of the IEA 15-megawatt offshore reference wind turbine. Tech. rep., Golden, CO (United States): National Renewable Energy Lab.(NREL); 2020.

[50] Martinez A, Iglesias G. Climate change impacts on wind energy resources in North America based on the CMIP6 projections. Sci Total Environ 2022;806:150580.

[51] Ibarra-Berastegi G, Ulazia A, Sáenz J, Serras P, Rojí SJG, Esnaola G, Iglesias G. The power flow and the wave energy flux at an operational wave farm: Findings from Mutriku, Bay of Biscay. Ocean Eng 2021;227:108654.

[52] Lobeto H, Menendez M, Losada IJ, Hemer M. The effect of climate change on wind-wave directional spectra. Glob Planet Change 2022;213:103820. http://dx.doi.org/10.1016/j.gloplacha.2022.103820.

[53] Zhou P, Yin P. An opportunistic condition-based maintenance strategy for offshore wind farm based on predictive analytics. Renew Sustain Energy Rev 2019;109:1–9.

[54] Liu Y. Introduction of the open-source boundary element method solver HAMS to the ocean renewable energy community. In: Proceedings of the European wave and tidal energy conference: EWTEC 2021. Technical Committee of the European Wave and Tidal Energy Conference (EWTEC); 2021.

[55] Liu Y, Yoshida S, Hu C, Sueyoshi M, Sun L, Gao J, Cong P, He G. A reliable open-source package for performance evaluation of floating renewable energy systems in coastal and offshore regions. Energy Convers Manage 2018;174:516–36.

[56] Sheng W, Tapoglou E, Ma X, Taylor CJ, Dorrell RM, Parsons DR, Aggidis G. Hydrodynamic studies of floating structures: Comparison of wave-structure interaction modelling. Ocean Eng 2022;249:110878.

[57] Zabala I, Pena-Sanchez Y, Kelly T, Henriques J, Penalba M, Faedo N, Ringwood J, Blanco JM. BEMRosetta: An open-source hydrodynamic coefficients converter and viewer integrated with Nemoh and FOAMM. 2021.

[58] Hall M, Housner S, Zalkind D, Bortolotti P, Ogden D, Barter G. An open-source frequency-domain model for floating wind turbine design optimization. In: Journal of physics: conference series, Vol. 2265. IOP Publishing; 2022, 042020.